



# Effect of the number of thiophene rings in polymers with 2,1,3-benzoxadiazole core on the photovoltaic properties



Thu Trang Do, Ye Eun Ha, Joo Hyun Kim\*

Department of Polymer Engineering, Pukyong National University, Yongdang-Dong, Nam-Gu, Busan 608-739, Republic of Korea

## ARTICLE INFO

### Article history:

Received 17 April 2013  
 Received in revised form 7 July 2013  
 Accepted 11 July 2013  
 Available online 26 July 2013

### Keywords:

Polymer solar cells  
 Thiophene  
 2,1,3-Benzoxadiazole  
 1,8-Diiodooctane  
 Morphology  
 Power conversion efficiency

## ABSTRACT

A series of polymers, poly{5,6-bis(decyloxy)-4-(thiophen-2-yl)benzo[c][1,2,5]oxadiazole} (1T-BO20), poly{4-(2,2'-bithiophen-5-yl)-5,6-bis(decyloxy)benzo[c][1,2,5]oxadiazole} (2T-BO20), poly{4-(2,2'-bithiophen-5-yl)-5,6-bis(decyloxy)-7-(thiophen-2-yl)benzo[c][1,2,5]oxadiazole} (3T-BO20) containing 2,1,3-benzoxadiazole derivative and different thiophene rings are synthesized. Effect of the number of thiophene rings on the optical, electrochemical and photovoltaic properties of the polymers is investigated. The maximum absorption wavelength and the optical band gap of the polymers are almost the same, indicating the polymers exhibit similar intramolecular charge transfer effect. The HOMO levels are in the order of 1T-BO20 (−5.60 eV) < 2T-BO20 (−5.45 eV) < 3T-BO20 (−5.36 eV), revealing that the HOMO level of the polymers are dependent of number of thiophene ring in the back bone. Under the illumination of AM 1.5G, 100 mW/cm<sup>2</sup>, the power conversion efficiency (PCE) of PSCs based on these polymers increases in the order of 1T-BO20 (1.66%), 2T-BO20 (1.71%) and 3T-BO20 (1.92%). Besides, we find that the efficiency of PSCs showed very different responses by the addition of DIO as a processing additive. The devices based on 1T-BO20 and 2T-BO20 with DIO exhibit an enhancement of PCE from 1.66% to 3.65% and from 1.71% to 2.40%, respectively, whereas PCE of the device based on 3T-BO20 with DIO decreased from 1.92% to 1.76%.

© 2013 Elsevier B.V. All rights reserved.

## 1. Introduction

Polymer solar cells (PSCs), especially bulk heterojunction (BHJ) PSCs comprising  $\pi$ -conjugated polymers and fullerene derivatives have attracted much interest in recent years due to their solution processability and flexibility, which potentially allow them to be manufactured using low-cost, high-throughput processes such as roll-to-roll printing and inkjet printing [1–3]. In the past years, poly(3-hexylthiophene) (P3HT) was used as the most common donor material because of its high carrier mobility [4,5]. However, the relatively large band gap of P3HT ( $E_g = 1.9$  eV) limits the harvest of photons from the solar spectrum. It is calculated that P3HT is only capable of absorbing about 46% of the available solar photons [6]

and only in the wavelength range between 350 nm and 650 nm. The limitation in the absorption is detrimental to the short circuit current ( $J_{sc}$ ) of the resulting photovoltaic cells as well as the high-lying HOMO energy level of P3HT limits the open circuit voltage ( $V_{oc}$ ) of its solar cell [7,8]. In recent years, the development of novel materials has contributed to significant improvements in device performance. Among various types of polymers, the conjugated polymers based on the alternating electron-rich and electron-deficient units along the polymer backbone have been shown to be able to achieve high power conversion efficiencies [9]. The state of internal charge transfer (ICT) transition from donor to acceptor inside the copolymer absorbs photons with long wavelengths which could extend the absorption and decrease the band gap of the copolymer [10].

Moreover, the morphology of the polymer:fullerene blend is a critical factor which affects the solar cell

\* Corresponding author. Tel.: +82 51 629 6452.  
 E-mail address: [jkim@pknu.ac.kr](mailto:jkim@pknu.ac.kr) (J.H. Kim).

performances [11,12]. Various methods have been developed to optimize the morphology such as thermal annealing [13–16], solvent annealing [17–19] and the use of co-solvents as the processing additives [20–22]. Considerable improvement of the PCE of PSCs by tuning the morphology of the active layers with various additives has been demonstrated and become a more attractive method due to its simplicity without an additional fabrication steps and production compatibility compared with thermal treatment [12,21,23,24]. They influence the size of the fullerene domains and enhance the crystallinity of the self-organized polymers by improving the solubility of the fullerenes and slightly elongating the drying time of the active layer [25].

Recently, 2,1,3-benzoxadiazole (BO) derivatives have been paid much attention as strong electron-deficient moieties used for PSC [26–29]. A BO possesses a high electron transporting ability due to two electron withdrawing imine (C = N) groups [30]. Besides, it also exhibits capability to adopt the quinoid structure in the polymer, resulting in a low band gap and coplanar polymer [27,29]. In comparison with a typical electron-withdrawing moiety 2,1,3-benzothiadiazole (BT), a BO has a low-lying oxidation potential which can decrease both the HOMO and LUMO energy levels [31]. The devices based on the polymers having BO moiety exhibit pretty high open circuit potentials [32]. Furthermore, it has been recently reported that the PCE of device based on copolymer PBDTBO containing benzo[1,2-*b*:4,5-*b'*]dithiophene and BO derivatives reached 5.7% [27]. Therefore polymers based on BO derivatives are potential photoactive material candidates for PSCs.

In this research, we synthesize two new  $\pi$ -conjugated alternating copolymers, poly{4-(2,2'-bithiophen-5-yl)-5,6-bis(decyloxy)benzo[c][1,2,5]oxadiazole} (2T-BO20), and poly{4-(2,2'-bithiophen-5-yl)-5,6-bis(decyloxy)-7-(thiophen-2-yl)benzo[c][1,2,5]oxadiazole} (3T-BO20), based on BO. The absorption, electrochemical and photovoltaic properties of 2T-BO20 and 3T-BO20 were explored and compared with that of poly{5,6-bis(decyloxy)-4-(thiophen-2-yl)benzo[c][1,2,5]oxadiazole} (1T-BO20) which was reported previously [28]. These polymers have similar structure but different number of thiophene rings in their repeat unit, one thiophene ring for 1T-BO20, two thiophene rings for 2T-BO20 and three thiophene rings for 3T-BO20. Thiophene was used because it has been shown to have relatively strong interchain interaction and high charge carrier mobility in BHJ type solar cells [10,33]. Furthermore, it has been reported that the optical and physical properties of copolymers can be controlled with suitable modification of thiophene conjugated length [34,35]. Therefore, we expected that an extension of thiophene ring can improve planarity and increase effective conjugation of polymer main chain which is translated into broader absorption and better photovoltaic performances [36]. In addition, these polymers are designed with two decyloxy chains on the 5- and 6-positions of BO unit to improve solubility of polymers in common organic solvents and make it more feasible to synthesize the polymers with high molecular weight. Herein, we will discuss the synthesis, characterization, and optical properties of the polymers as well as the photovoltaic properties of the devices based on these polymers. On the other hand, the influence of the

number of thiophene rings and DIO as the processing additive will be studied.

## 2. Experimental section

### 2.1. Materials

Methylene chloride (MC) was distilled over CaH<sub>2</sub>. All other chemicals were purchased from Sigma-Aldrich Co., Tokyo Chemical Industry (TCI) or Alfa Aesar (A Johnson Matthey Company) and used as received unless otherwise described.

### 2.2. Synthesis of monomers and polymers

#### 2.2.1. Synthesis of 1,2-bis(decyloxy)-benzene (2)

Sodium hydroxide (NaOH, 3.56 g, 89.1 mmol) was dissolved in methanol (100 mL) at 0 °C for 30 min and then catechol (4.46 g, 40.5 mmol) was added slowly. White solution turned to deep green and finally dark. At this time 1-bromodecane (19.7 g, 89.1 mmol) was added into the mixture dropwise and then the mixture was refluxed under the nitrogen atmosphere. After 8 h, reaction mixture was cooled down to room temperature and then the solvent was removed under the reduced pressure. A portion of 250 mL of water was added into a reaction mixture and then the organic layer was extracted using a portion of 250 mL of ethyl acetate (EA). The organic layer was dried over anhydrous magnesium sulfate (MgSO<sub>4</sub>) and the solvent was removed using a rotary evaporator. The combined organic layer was triturated from MC and methanol to gain the off-white solid (11.7 g, 73.8%). mp: 40.3 °C. <sup>1</sup>H NMR (400 MHz, CDCl<sub>3</sub>, ppm):  $\delta$  6.87 (s, 4H), 3.99–3.95 (t, *J* = 7.0 Hz, 4H), 1.83–1.76 (m, 4H), 1.48–1.41 (m, 4H), 1.33–1.26 (m, 24H), 0.88–0.85 (t, *J* = 7.0 Hz, 6H). <sup>13</sup>C NMR (100 MHz, CDCl<sub>3</sub>, ppm):  $\delta$  150.29, 122.34, 115.46, 65.81, 32.89, 30.24, 30.51, 30.44, 30.19, 29.65, 26.09, 23.67, 15.05.

#### 2.2.2. Synthesis of 1,2-dinitro-4,5-bis(decyloxy)-benzene (3)

Compound 2 (9.57 g, 24.5 mmol) was dissolved in MC (150 mL) and acetic acid (AcOH, 150 mL). A portion of 28.5 mL of nitric acid (HNO<sub>3</sub>, 65.0%) was added dropwise into a reaction mixture at 10 °C. The reaction was allowed to warm to room temperature and stirred for 1 h. The mixture was again cooled to 10 °C and 65.5 mL of 95.0% HNO<sub>3</sub> was added dropwise into a reaction mixture. The mixture was allowed to warm to room temperature and the mixture was stirred for 24 h. After completion of the reaction, the reaction mixture was poured into ice-water and the MC layer separated. The water phase was extracted with MC. The combined organic layer was washed with water, aqueous solution of NaHCO<sub>3</sub>, brine and dried over anhydrous MgSO<sub>4</sub> and then removed using a rotary evaporator. The crude product was recrystallized from methanol. The yellow solid product yield was 10.4 g (88.3%). mp: 83.5 °C. <sup>1</sup>H NMR (400 MHz, CDCl<sub>3</sub>, ppm):  $\delta$  7.27 (s, 2H), 4.09–4.06 (t, *J* = 6.5 Hz, 4H), 1.88–1.81 (m, 4H), 1.49–1.42 (m, 4H), 1.34–1.25 (m, 24H), 0.87–0.84 (t, *J* = 6.5 Hz, 6H). <sup>13</sup>C NMR (100 MHz, CDCl<sub>3</sub>, ppm):  $\delta$  152.81, 137.48, 108.92, 71.20, 32.87, 30.55, 30.51, 30.30, 30.21, 29.69, 26.80, 23.66, 15.07.

### 2.2.3. Synthesis of 5,6-bis-decyloxy-benzo[c][1,2,5]oxadiazole (4)

A mixture of compound 3 (9.85 g, 20.5 mmol), sodium azide (NaN<sub>3</sub>, 6.69 g, 103 mmol), and tetrabutyl ammonium bromide (*n*-Bu<sub>4</sub>NBr, 1.32 g, 4.10 mmol) was heated under reflux in toluene (100 mL) for 12 h under N<sub>2</sub> atmosphere. A portion of 6.45 g of triphenylphosphine (PPh<sub>3</sub>, 24.6 mmol) was added in small portions into a reaction mixture. After completion of addition of PPh<sub>3</sub>, the mixture was heated under reflux for an additional 24 h. The reaction mixture was cooled to room temperature and the organic solvent was removed under the reduced pressure. The crude product was purified by silica gel column eluting with MC:hexane (1:10 v/v). The yellow solid yield was 5.25 g (59.2%). mp: 110.7 °C. <sup>1</sup>H NMR (400 MHz, CDCl<sub>3</sub>, ppm): δ 6.78 (s, 2H), 4.06–4.02 (t, *J* = 6.6 Hz, 4H), 1.90–1.83 (m, 4H), 1.51–1.44 (m, 4H), 1.35–1.25 (m, 24H), 0.87–0.84 (t, *J* = 6.6 Hz, 6H). <sup>13</sup>C NMR (100 MHz, CDCl<sub>3</sub>, ppm): δ 156.19, 147.82, 91.66, 70.35, 32.89, 30.57, 30.53, 30.32, 30.28, 29.58, 26.96, 23.66, 15.08.

### 2.2.4. Synthesis of 4,7-dibromo-5,6-bis-decyloxy-benzo[c][1,2,5]oxadiazole (5)

A portion of 14.5 g of bromine (90.6 mmol) was added into a solution of compound 4 (5.41 g, 12.5 mmol) in MC/ acetic acid (200 mL/100 mL) at room temperature. The resulting mixture was stirred in the dark for ca. 3 days at room temperature. A portion of 200 mL of aqueous NaOH solution (10.0 g in 200 mL) was slowly added into the reaction mixture. The aqueous phase was extracted with 100 mL of MC 3 times then the combined organic layer was dried over anhydrous MgSO<sub>4</sub> and concentrated under reduced pressure to afford a crude solid. The crude product was purified through column chromatography (SiO<sub>2</sub>, hexane:MC (9:1 v/v)). The white solid product yield was 5.62 g (76.2%). mp: 52.4 °C. <sup>1</sup>H NMR (400 MHz, CDCl<sub>3</sub>, ppm): δ 4.13–4.10 (t, *J* = 6.6 Hz, 4H), 1.87–1.80 (m, 4H), 1.52–1.45 (m, 4H), 1.34–1.25 (m, 24H), 0.87–0.84 (t, *J* = 6.2 Hz, 6H). <sup>13</sup>C NMR (100 MHz, CDCl<sub>3</sub>, ppm): δ 156.66, 148.44, 100.55, 76.39, 32.88, 31.18, 30.56, 30.55, 30.36, 30.30, 26.88, 23.66, 15.09.

### 2.2.5. Synthesis of 5,6-bis-decyloxy-4,7-di(thien-2-yl)benzo[c][1,2,5]oxadiazole (6)

Compound 5 (5.61 g, 9.50 mmol), 2-tributylstannylthiophene (8.84 g, 23.7 mmol), [1,1'-bis(diphenylphosphino)ferrocene] dichloropalladium (II), complex with dichloromethane (Pd(dppf)Cl<sub>2</sub>·CH<sub>2</sub>Cl<sub>2</sub>, 0.39 g, 0.48 mmol) were dissolved in dry toluene (50.0 mL) and then the reaction mixture was heated under reflux for overnight under N<sub>2</sub> atmosphere. After the reaction mixture was cooled to room temperature, water and EA were added. The aqueous phase was extracted with 100 mL of EA 3 times and combined organic layer was dried over anhydrous MgSO<sub>4</sub>. The solvent was removed under the vacuum and the residue was purified by column chromatography (SiO<sub>2</sub>, hexane:chloroform, 10:1 (v/v)) afforded a yellow solid (3.81 g, 67.2%). mp: 84.2 °C. <sup>1</sup>H NMR (400 MHz, CDCl<sub>3</sub>, ppm): δ 8.45–8.44 (dd, *J*<sub>1</sub> = 1.1 Hz, *J*<sub>2</sub> = 3.7 Hz, 2H), 7.49–7.41 (dd, *J*<sub>1</sub> = 1.1 Hz, *J*<sub>2</sub> = 5.2 Hz, 2H), 7.21–7.19 (t, 4.6 Hz, 2H), 4.15–4.11 (t, *J* = 11.0 Hz, 4H), 2.02–1.94 (m, 4H), 1.48–1.41 (m, 4H),

1.37–1.26 (m, 24H), 0.89–0.85 (t, *J* = 6.6 Hz, 6H). <sup>13</sup>C NMR (100 MHz, CDCl<sub>3</sub>, ppm): δ 152.69, 147.74, 133.90, 131.85, 129.00, 128.14, 114.05, 75.50, 32.92, 31.28, 30.62, 30.58, 30.56, 30.35, 26.88, 23.69, 15.11.

### 2.2.6. Synthesis of 4,7-bis(5-bromothiophen-2-yl)-5,6-bis-decyloxy-benzo[c][1,2,5]oxadiazole (7)

A portion of *N*-bromosuccinimide (NBS, 2.81 g, 15.8 mmol) was added portion wise into a solution of compound 6 (3.76 g, 6.30 mmol) in 40.0 mL of *N,N*-dimethylformamide (DMF) in ice bath. After addition of NBS, the reaction mixture was stirred in the dark for 24 h and the temperature being gradually raised to room temperature. A portion of aqueous sodium bisulfite (NaHSO<sub>3</sub>, 5 wt.%) was added into the reaction mixture and stirred for 20 min to remove excess of NBS. The mixture was then extracted with 100 mL of EA. The organic layer was combined and dried over anhydrous MgSO<sub>4</sub>. The organic solvent was removed under the reduced pressure. The residue solid was purified by flash chromatography on silica gel column eluting with MC:hexane (1:10 v/v). The reddish orange solid product yield was 4.21 g (88.6%). mp: 76.7 °C. <sup>1</sup>H NMR (400 MHz, CDCl<sub>3</sub>, ppm): δ 8.22–8.21 (d, *J* = 4.0 Hz, 2H), 7.15–7.14 (d, *J* = 4.4 Hz, 2H), 4.15–4.11 (t, *J* = 7.4 Hz, 4H), 2.0–1.93 (m, 4H), 1.47–1.41 (m, 4H), 1.36–1.27 (m, 24H), 0.89–0.85 (t, *J* = 6.6 Hz, 6H). <sup>13</sup>C NMR (100 MHz, CDCl<sub>3</sub>, ppm): δ 152.27, 147.23, 135.31, 132.21, 131.09, 117.39, 113.71, 75.83, 32.99, 31.24, 30.09, 30.65, 30.55, 30.43, 26.89, 23.77, 15.19.

### 2.2.7. General procedure for Stille polymerization

2.2.7.1. Poly{5,6-bis(decyloxy)-4-(thiophen-2-yl)benzo[c][1,2,5]oxadiazole} (1T-BO20). Compound 5 (148 mg, 0.25 mmol), 2,5-bis(trimethylstannyl)thiophene (102 mg, 0.25 mmol), Pd<sub>2</sub>dba<sub>3</sub> (11.4 mg, 12.5 μmol) and tri-(*o*-tolyl)phosphine (30.4 mg, 100 μmol) were mixed in dry degassed toluene (6.0 mL). The reaction mixture was heated to reflux for 48 h under nitrogen. After cooling to room temperature, the mixture was poured into 200 mL methanol and the polymer was allowed to precipitate. The polymer was filtered and purified by Soxhlet extraction using methanol, hexane and chloroform. The chloroform fraction was concentrated by rotary evaporator and then poured into methanol to precipitate again. The polymer was filtered and dried in vacuum to give 1T-BO20 (89.3 mg, 69.6%) as black solid. <sup>1</sup>H NMR (400 MHz, CDCl<sub>3</sub>, ppm): δ 8.67–8.24 (br, 2H), 4.43–4.21 (br, 4H), 2.26–2.18 (br, 4H), 2.13–1.97 (br, 4H), 1.61–1.40 (br, 4H), 1.31–1.23 (br, 20H), 0.86–0.84 (br, 6H).

2.2.7.2. Poly{4-(2,2'-bithiophen-5-yl)-5,6-bis(decyloxy)benzo[c][1,2,5]oxadiazole} (2T-BO20). 2T-BO20 was synthesized by the Stille coupling reaction between compound 5 (148 mg, 0.25 mmol) and 5,5'-bis(trimethylstannyl)-2,2'-bithiophene (123 mg, 0.25 mmol). The same reaction condition and procedure were used as in the polymerization of 1T-BO20. The yield of the polymer was 63.1 mg (42.4%) as black solid. <sup>1</sup>H NMR (400 MHz, CDCl<sub>3</sub>, ppm): δ 8.46–7.94 (br, 4H), 4.25–4.06 (br, 4H), 2.21–2.01 (br, 4H), 1.57–1.46 (br, 4H), 1.44–1.17 (br, 24H), 0.91–0.82 (br, 6H).

2.2.7.3. Poly{4-(2,2'-bithiophen-5-yl)-5,6-bis(decyloxy)-7-(thiophen-2-yl)benzo[c][1,2,5]oxadiazole} (3T-BO20). 3T-BO20 was synthesized by the Stille coupling reaction between compound **7** (189 mg, 0.25 mmol) and 2,5-bis(trimethylstannyl)thiophene (103 mg, 0.25 mmol). The same reaction condition and procedure were used as in the polymerization of 1T-BO20. The yield of the polymer was 82.6 mg (48.8%).  $^1\text{H NMR}$  (400 MHz,  $\text{CDCl}_3$ , ppm):  $\delta$  8.52–7.82 (br, 4H), 7.02–6.53 (br, 2H), 4.43–3.92 (br, 4H), 2.37–2.14 (br, 4H), 2.07–1.91 (br, 4H), 1.59–1.17 (br, 24H), 0.98–0.79 (br, 6H).

### 2.3. Measurements

Synthesized compounds were characterized by  $^1\text{H NMR}$  and  $^{13}\text{C NMR}$  spectrum, which were obtained with a JEOL JNM ECP-400 spectrometer. Melting point of compounds was measured by MPA100 OptiMelt Automated Melting Point System with heating rate of  $10\text{ }^\circ\text{C}/\text{min}$ . The gel permeation chromatography (GPC) measurements were conducted by GPC system equipped with a Varian 212-LC pump, a Rheodyne 6-port sample injection valve, a Waters Temperature Control Module, a Waters 410 differential RI detector and two Waters Styragel HR4E columns using polystyrene as standard and toluene as eluent. The thermogravimetric analysis (TGA) was carried out under the  $\text{N}_2$  atmosphere at a heating rate of  $10\text{ }^\circ\text{C}/\text{min}$  with a Perkin-Elmer TGA 7 thermal analyzer. The UV-Vis spectrum was recorded using a JASCO V-530 UV-Vis Spectrophotometer. The cyclic voltammetry (CV) was performed by an Ivium B14406 with a three electrode cell in a 0.1 M *n*-tetrabutylammonium hexafluorophosphate (*n*-Bu $_4$ NPF $_6$ ) acetonitrile solution at a scan rate of 100 mV/s. A Pt coil was used as the counter electrode and dip-polymer on a Pt wire was used as the working and a Ag/Ag $^+$  electrode was used as the reference electrode. Atomic Force Microscope (AFM) images were taken on a Digital Instruments (USA), Multi Mode $^{\text{TM}}$  SPM. The AFM images were obtained by the tapping mode and a scan rate of 2 Hz. The *J*-*V* measurements under the 1.0 sun ( $100\text{ mW}/\text{cm}^2$ ) condition from a 150 W Xe lamp with an AM 1.5G filter were performed using a KEITHLEY Model 2400 source-measure unit. A calibrated Si reference cell with a KG5 filter certified by National Institute of Advanced Industrial Science and Technology was used to confirm 1.0 sun condition. The thickness of films was measured by an Alpha-Step IQ surface profiler (KLA-Tencor Co.).

### 2.4. Fabrication of PSCs

PSCs were fabricated in the configuration of the common sandwich structure: ITO/PEDOT:PSS/active layer (polymer: [6,6]-phenyl-C61-butyric acid methyl ester (PCBM))/Al. The ITO-coated glass substrates were cleaned with deionized water, acetone, methanol, 2-propanol in an ultrasonic bath. After the substrates were dried, they were treated with UV/O $_3$  for 120 s prior to use. A layer of poly(3,4-ethylenedioxythiophene):poly(styrenesulfonate) (PEDOT:PSS, Celvios P) with 2-propanol (IPA) (PEDOT:PSS/IPA = 1/2 by volume) was deposited onto the ITO substrate (sheet resistance =  $15\ \Omega/\text{sq}$ ) with a thickness of ca. 40 nm by spin-coating

and followed by baking at  $150\text{ }^\circ\text{C}$  for 10 min under the ambient condition. The active layer was spin-cast from the blend solution of polymer/PCBM (5 mg of polymer and 10 mg of PCBM were dissolved in 1 mL chloroform (CF) with or without 1,8-diiodooctane (DIO) (1 vol%). Prior to spin coating, the active solution was filtered through a  $0.45\ \mu\text{m}$  membrane filter. Then, the aluminum cathode deposited with a thickness of 110 nm through a shadow mask with a device area of  $0.13\ \text{cm}^2$  at  $2 \times 10^{-6}$  Torr.

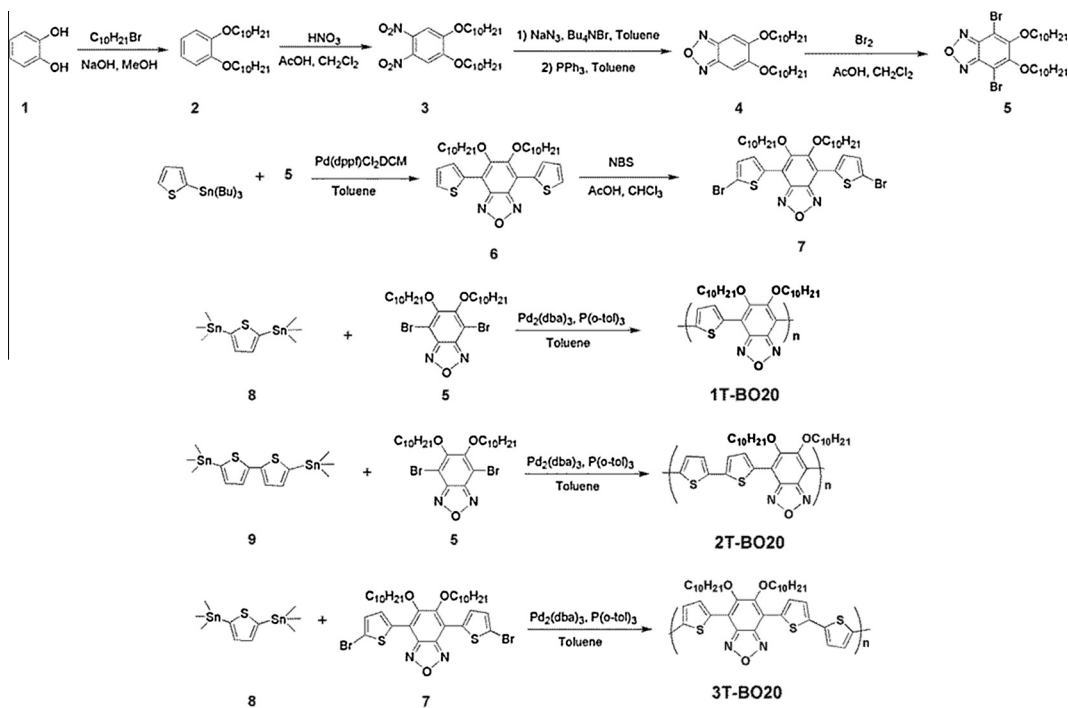
## 3. Results and discussion

### 3.1. Synthesis and characterization

Scheme 1 shows the general synthetic route for monomers and polymers. Compound **2** was prepared by alkylation of catechol with 1-bromodecane in methanol and sodium hydroxide at  $80\text{ }^\circ\text{C}$ . Compound **3**, **4**, **5**, **6** and **7** were synthesized by the reported procedures [26]. The polymers (1T-BO20, 2T-BO20 and 3T-BO20) were synthesized by the typical Stille coupling reaction. The molecular weight of the polymers was determined by the gel permeation chromatography (GPC) relative to polystyrene standards by using a toluene eluent. The number average molecular weight ( $M_n$ ) of 1T-BO20, 2T-BO20 and 3T-BO20 was 68500, 11500, and 36600 g/mol, respectively; with polydispersity index (PDI) of 1.73, 7.61, and 1.66, respectively. The thermal stability of the polymers was determined by the thermogravimetric analysis (TGA). As shown in Fig. 1, 1T-BO20, 2T-BO20 and 3T-BO20 were thermally stable up to 308, 279, and  $309\text{ }^\circ\text{C}$ . A temperature of 5%-weight loss in TGA thermogram of 1T-BO20, 2T-BO20 and 3T-BO20 were 308, 279, and  $309\text{ }^\circ\text{C}$ , respectively. Among the polymers, 2T-BO20 exhibit lower thermal stability. This is presumably due to its lower molecular weight than that of the others. The thermal stability of the resulting polymers prevents degradation of the active layer during fabrication of PSCs [37,38].

### 3.2. Optical and electrochemical properties

Fig. 2 shows the UV-Vis absorption spectra of 1T-BO20, 2T-BO20 and 3T-BO20 films. The optical properties are summarized in Table 1. All of the absorption spectra were exhibited two broad absorption bands near 310–460 nm and 460–740 nm. The former corresponds to localized  $\pi$ - $\pi$  transition of the conjugated polymer backbone and the latter corresponds to intramolecular charge transfer (ICT) between the electron rich thiophene ring(s) and electron deficient BO unit. The absorption spectrum of 1T-BO20 resembles that of PTTTBO [28] whose structure is similar to 1T-BO20. The maximum absorption peaks at longer wavelength region of 1T-BO20 film ( $\lambda_{\text{max}} = 608, 662\text{ nm}$ ) show red-shift of 6, 11 nm compared to those of 3T-BO20 ( $\lambda_{\text{max}} = 602, 653\text{ nm}$ ). Whereas the maximum absorption peaks at longer wavelength region of 2T-BO20 ( $\lambda_{\text{max}} = 611, 661\text{ nm}$ ) are similar to those of 1T-BO20. This is because of the similar chemical structural feature of the three polymers resulting in similar ICT effect. The maximum absorption peak at shorter wavelength region of 2T-BO20



Scheme 1. Synthesis route of monomers and polymers.

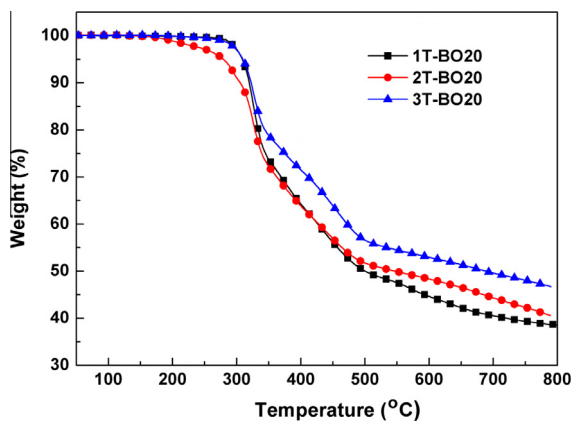


Fig. 1. TGA thermograms of polymers.

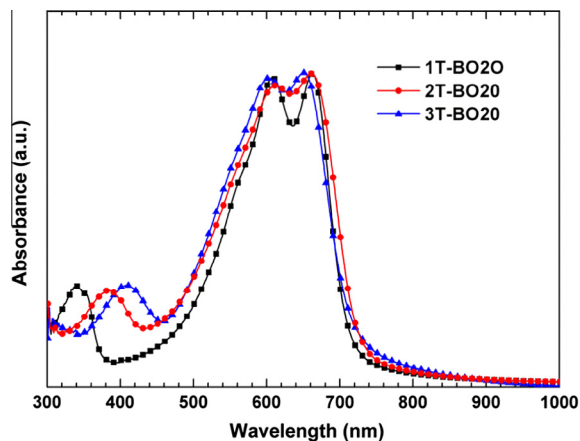


Fig. 2. UV-Vis absorption spectra of polymers.

(383 nm) and 3T-BO20 (408 nm) are red-shifted of 44 and 69 nm, than 1T-BO20 (339 nm). In addition, the absorption range at the longer wavelength region of the polymers becomes broader as increases the number of thiophene rings. This means that the effective conjugation length increases with the increasing number of the thiophene rings in a repeat unit, which leads red-shift of the absorption spectrum of the polymer and thereby increases photon harvesting [39]. Interestingly, there is one other example with opposite effect: after adding the thiophene rings into polymer backbones lead to a blue shift in the absorption spectrum [40]. This might be the result of decrease in the degree of ICT between donor and acceptor. The optical band gap ( $E_{g,opt}$ ) of 1T-BO20, 2T-BO20 and 3T-BO20 estimated from

the absorption edges in the UV-Vis spectra were 1.73 eV. As expected, the low  $E_{g,opt}$  of BO-based alternating copolymers, which is lower than that of P3HT (~2.0 eV) and is originated from the strong  $\pi$ - $\pi$  stacks and the ICT absorption bands [41,42].

To understand the energy levels of the polymers, and expect the parameters of the resulting solar cells, it is necessary to determine the HOMO and LUMO level of the polymers. Thus, the electrochemical behaviors of the polymers were investigated by CV measurements (See Fig. 3) were carried out in anhydrous acetonitrile solution containing 0.1 M  $Bu_4NPF_6$  as the supporting electrolyte. The reference electrode ( $Ag/Ag^+$ ) was calibrated by the

**Table 1**

Optical absorption and electrochemical properties of polymers.

Polymers	$\lambda_{\max}$ (nm)	$E_{g,\text{opt}}$ (eV) <sup>a</sup>	HOMO (eV) <sup>b</sup>	LUMO (eV) <sup>c</sup>	$E_{g,\text{cv}}$ (eV) <sup>d</sup>
1T-BO20	608, 662	1.73	−5.60	−3.87	1.93
2T-BO20	611, 661	1.73	−5.45	−3.72	1.94
3T-BO20	602, 653	1.73	−5.36	−3.63	1.82

<sup>a</sup> The optical band gap was obtained from the equation  $E_{g,\text{opt}} = 1240/\lambda_{\text{edge}}$ , where  $\lambda_{\text{edge}}$  is the onset value of absorption spectrum in long wavelength direction.

<sup>b</sup> Calculated from the oxidation onset potential.

<sup>c</sup> Calculated from the HOMO and optical band gap energy (LUMO = HOMO +  $E_{g,\text{opt}}$ ).

<sup>d</sup> The electrochemical band gap was calculated according the equation:  $E_{g,\text{cv}} = \text{oxidation onset potential} - \text{reduction onset potential}$ .

ferrocene/ferrocenium (Fc/Fc<sup>+</sup>) redox couple (4.8 eV below the vacuum level). From the values of the onset of oxidation potentials of the polymers, the HOMO levels of the polymers are estimated. The estimated HOMO and LUMO energy levels of the polymers were compiled in Table 1. The HOMO energy levels of the polymers were in the order of 1T-BO20 (−5.60 eV) < 2T-BO20 (−5.45 eV) < 3T-BO20 (−5.36 eV). Thiophene is very strong electron donor and has a high-lying ionization potential so that the HOMO energy level depends on the number of thiophene rings in the polymer. These data agree with previously published reports demonstrating that adding more thiophene rings resulted in a higher HOMO energy level [42,43]. Besides, the relatively low HOMO levels of these polymers promise higher the  $V_{\text{oc}}$  values of the photovoltaic cells compared to that of P3HT:PCBM based device. The electrochemical band gap ( $E_{g,\text{cv}}$ ) of 1T-BO20, 2T-BO20 and 3T-BO20 were estimated from the difference between onset potential of reduction and oxidation, which are 1.93, 1.94 and 1.82 eV, respectively, which are quite different from the  $E_{g,\text{cv}}$  of the polymers. This discrepancy might have been caused by the presence of an energy barrier at the interface between the polymer film and the electrode surface [44–46]. Similar phenomena have been reported for other polymer systems [47]. It was found that, although the HOMO and LUMO energy levels of these polymers are quite different, they have the same optical band gap. This possibly due to the addition of thiophene ring(s) concurrently pulled the HOMO and LUMO energy levels up. Beside, as discussed

above, three polymers have almost the same features in the long wavelength region.

### 3.3. Photovoltaic properties

The photovoltaic performances of polymers were investigated in PSCs having the sandwich structure of ITO/PEDOT:PSS/polymer:PCBM/Al. Fig. 4 shows the typical  $J$ - $V$  curves of polymer:PCBM devices in the dark and under the illumination of AM 1.5G, 100 mW/cm<sup>2</sup> without DIO. The photovoltaic parameters of the devices are summarized in Table 2. The devices prepared from PCBM blended with 1T-BO20, 2T-BO20 or 3T-BO20 exhibited  $V_{\text{oc}}$  of 0.82, 0.82, and 0.73 V, respectively, which are related with the HOMO energy level of the polymers [48] and the difference between the HOMO energy level of the polymer and the LUMO of PCBM. The device with 1T-BO20 exhibited a higher  $V_{\text{oc}}$  than that of the device based on 3T-BO20 which benefits from its a lower-lying HOMO energy level. Surprisingly, the devices based on 2T-BO20 and 1T-BO20 have the same  $V_{\text{oc}}$  value, even though 2T-BO20 has higher-lying HOMO energy level. This might be ascribed to the difference in  $V_{\text{oc}}$  of devices is not only affected by their HOMO levels but also other factors such as morphology and carrier recombination rate [49]. The  $J_{\text{sc}}$  values of the devices with the 1T-BO20, 2T-BO20 and 3T-BO20 films were 4.74, 3.39 and 4.98 mA/cm<sup>2</sup>, respectively. When 1T-BO20 based device compared to the device based on 3T-BO20, with increasing of thiophene rings in the polymer backbone,

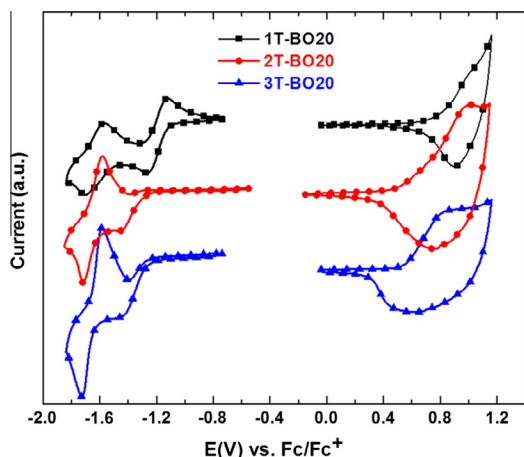


Fig. 3. Cyclic voltammograms of polymers.

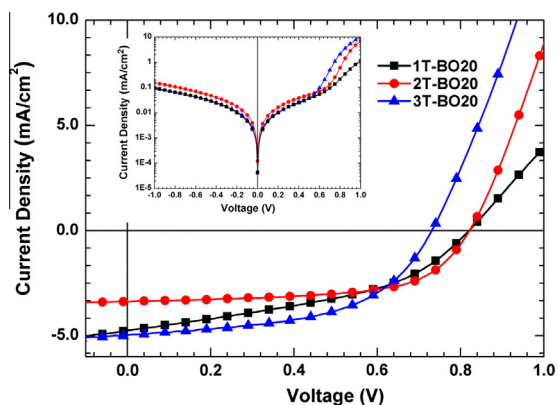


Fig. 4.  $J$ - $V$  curves of PSCs based on 1T-BO20, 2T-BO20 and 3T-BO20 in the dark condition (inset) and under the illumination of AM 1.5G, 100 mW/cm<sup>2</sup>.

**Table 2**

Photovoltaic parameters of PSCs based on polymers:PCBM blend films.

Active layer polymer/PCBM	Thickness (nm)	$J_{sc}$ (mA/cm <sup>2</sup> )	$V_{oc}$ (V)	FF (%)	PCE (%)	$R_s$ ( $\Omega$ cm <sup>2</sup> )	$R_p$ (k $\Omega$ cm <sup>2</sup> )
1T-BO20	150	4.74	0.82	42.7	1.66	10.5	10.7
1T-BO20 <sup>a</sup>	115	8.37	0.85	48.0	3.65	3.29	57.9
2T-BO20	125	3.39	0.82	61.5	1.71	7.03	6.64
2T-BO20 <sup>a</sup>	145	5.55	0.82	52.8	2.40	2.36	29.7
3T-BO20	120	4.98	0.73	52.8	1.92	9.06	11.2
3T-BO20 <sup>a</sup>	125	4.30	0.79	51.9	1.76	12.6	24.6

<sup>a</sup> DIO was added for additive.

the  $J_{sc}$  slightly increased. However, in case of 2T-BO20, with increasing the thiophene ring in the polymer compared to that of 1T-BO20, the  $J_{sc}$  decreased; even though absorption spectrum of 2T-BO20 is red-shifted compared to that of 1T-BO20. This is probably the result of lower molecular weight of 2T-BO20 compared to that of 1T-BO20. It has been reported that the low  $J_{sc}$  of solar cells fabricated using a low molecular weight polymer originates mainly from the reduced charge carriers mobility in the donor phase of the heterojunction [50,51]. The FF values of device based on 1T-BO20, 2T-BO20 and 3T-BO20 were 42.7%, 61.5% and 52.8%, respectively. We can recognize that 2T-BO20 showed the highest FF. It was possibly due to the good contact between layers of device which possessed the lowest series resistance ( $R_s$ ) value compared to those of 1T-BO20 and 3T-BO20. It has been reported that FF of the devices is more sensitive to the polymer–metal interface morphology unlike other parameters [52]. Therefore, the low molecular weight of 2T-BO20 not seemed to be much effect on FF. The PCE of 1T-BO20, 2T-BO20 and 3T-BO20 based devices were 1.66%, 1.71% and 1.92%, respectively. This result indicates that modification polymer structures by introducing thiophene rings into polymer back bone to increase  $\pi$ -conjugated length and improve planarity could lead to improve performances of solar cell devices. The similar results have been reported for other polymer systems [39,42,53]. Interestingly, adding thiophene rings into polymer based on 2,1,3-benzothiadiazole [54] whose structures are similar to our research showed the opposite results with ours. The absorption wavelength was blue shifted and performances of device decreased.

In order to further optimized photovoltaic performance, we added 1% (by volume) DIO as additive to the solution of the blend to examine its effect on the performance of the devices. We found that after adding DIO, the devices based on 1T-BO20 and 2T-BO20 exhibited significantly increased PCEs, which are 3.65% and 2.40%, respectively. This result revealed that DIO impacted on the morphology of active layer and it benefits for the exciton dissociation and carrier collection efficiency, thus leading to an increase in the short-circuit current density as well as the device efficiency [55]. Interestingly, the device of 3T-BO20 showed a very different response to the addition of DIO compared to 1T-BO20 and 2T-BO20. This polymer gave better performances without adding DIO. The  $J_{sc}$  and PCE of the device based on 3T-BO20 decreased to 4.30 mA/cm<sup>2</sup> and 1.76%, respectively. The low  $J_{sc}$  obtained for this polymer possibly due to the morphology not being fully optimized through the addition of DIO [56] or 3T-BO20 has already reached

the optimal morphology in the blend without DIO [55]. As for the device with DIO, the  $V_{oc}$  of the device based on 1T-BO20, 2T-BO20, and 3T-BO20 were 0.85, 0.82, 0.79 V, which are strongly related with the HOMO energy level of the polymers.

To investigate the effects of the additives on the surface morphology, we obtained the images by a atomic force microscopy (AFM). Fig. 6 shows the surface topography of BHJ films as directly measured from the same solar cell devices before and after the incorporation of DIO referred to in Figs. 4 and 5, respectively. As shown in Fig. 6 without DIO, the root-mean-square roughness (r.m.s.) of the 1T-BO20/PCBM, 2T-BO20/PCBM and 3T-BO20/PCBM films were 7.48, 3.98 and 5.66 nm, respectively. However, when DIO was used, the r.m.s. values of the blend films increased to 10.72, 5.89 and 11.54 nm for the films of 1T-BO20/PCBM, 2T-BO20/PCBM and 3T-BO20/PCBM, respectively. The morphology of 1T-BO20/PCBM film processed with DIO (Fig. 6b) showed larger scale phase separation and higher surface roughness than that in the BHJ film made without processing additive. Because of the more optimized morphology, this polymer showed significant enhancement of  $J_{sc}$  and FF, which lead to an increase in PCE [55]. In case of 2T-BO20/PCBM blend film with DIO, a significant reduction in phase separation and small domain size is observed in Fig. 6d. The morphology of this blend film was more uniform than that of 2T-BO20/PCBM blend film without DIO. Besides, there is no large phase separation, showing good miscibility between 2T-BO20 and PCBM [57]. This leads to a large interface for exciton

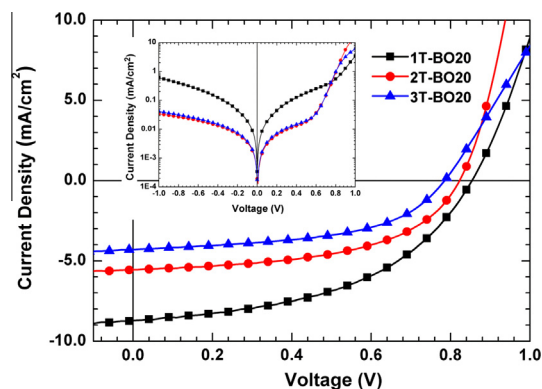


**Fig. 5.**  $J$ - $V$  curves of PSCs based on 1T-BO20, 2T-BO20 and 3T-BO20 with 1% DIO in the dark condition (inset) and under the illumination of AM 1.5G, 100 mW/cm<sup>2</sup>.

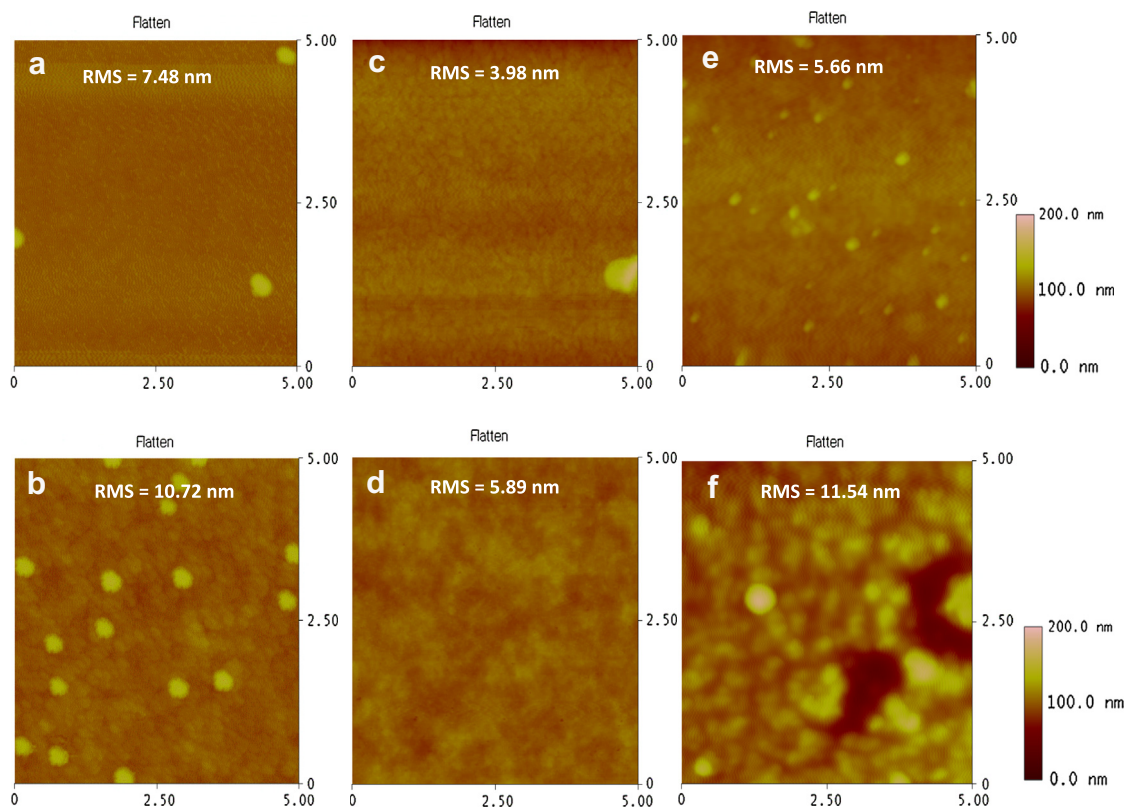


**Fig. 6.** AFM height images of polymer:PCBM blend films: (a) 1T-BO20 without DIO; (b) 1T-BO20 with 1% DIO; (c) 2T-BO20 without DIO; (d) 2T-BO20 with 1% DIO; (e) 3T-BO20 without DIO and (f) 3T-BO20 with 1% DIO (size:  $5 \mu\text{m} \times 5 \mu\text{m}$ ).

dissociation and bicontinuous interpenetrating networks for free charge transportation, which is well consistent with the improved  $J_{sc}$  in devices [58]. In contrast, the blend film of 3T-BO20/PCBM with DIO (Fig. 6f) exhibited rough morphology and much larger domain size with a r.m.s. of 11.54 nm indicating large phase separation took place. The severe phase separation in active layer reduces the area for charge separation and increases the recombination of excitons, leading to low photocurrent I [2].

#### 4. Conclusions

We have demonstrated that the modification in chemical structure of conjugated polymers by adding thiophene rings into polymer back bone could lead to change in optical, electrochemical, and photovoltaic properties. The maximum absorption wavelength and the band gap of the polymers were almost the same because the polymers exhibited similar ICT effect. However, there are some reports showed the opposite results to ours. Adding thiophene rings into polymer back bones could lead to blue shifted absorption [40,54]. Therefore, it is necessary to investigate more examples to study these phenomena. Thiophene is very strong electron donor and has a high-lying ionization potential so that the HOMO energy levels of the polymers depend on the number of thiophene rings in the polymer. The polymer (3T-BO20) containing three thiophene rings in a repeat unit showed the best photovoltaic performances compared to those of 1T-BO20 and 2T-BO20.

The PCE,  $V_{oc}$ ,  $J_{sc}$  and FF of the device based on 3T-BO20 were 1.92%, 0.73 V, 4.98  $\text{mA}/\text{cm}^2$  and 52.8%, respectively. This study also revealed the different effect trend in film morphology and performances of devices based on these polymer:PCBM blends when using DIO as a processing additive. Both of polymers 1T-BO20 and 2T-BO20 based devices exhibited an enhancement of PCE from 1.66% to 3.65% and from 1.71% to 2.40%, respectively; whereas 3T-BO20 gave the best performance without DIO. The PCE of device based on 3T-BO20 reduced from 1.92% to 1.76% by the addition of DIO. This result implies that number of thiophene rings in polymer back bones may reduce the positive effect of additives for optimum control of the nanomorphology.

#### Acknowledgments

This work was financially supported by Converging Research Center Program through the Ministry of Education, Science and Technology (2012K001279) and Basic Science Research Program through the National Research Foundation of Korea (NRF) funded by the Ministry of Education, Science and Technology (2013020225).

#### References

- [1] Y. Liang, Y. Wu, D. Feng, S.T. Tsai, H.J. Son, G. Li, L. Yu, *J. Am. Chem. Soc.* 131 (2009) 56–57.
- [2] E. Wang, L. Hou, Z. Wang, Z. Ma, S. Hellström, W. Zhuang, F. Zhang, O. Inganäs, M.R. Andersson, *Macromolecules* 44 (2011) 2067–2073.

- [3] E. Zhou, J. Cong, K. Tajima, C. Yang, K. Hashimoto, J. Phys. Chem. C 116 (2012) 2608–2614.
- [4] M.R. Reyes, K. Kim, D.L. Carroll, Appl. Phys. Lett. 87 (2005) 083506.
- [5] J.Y. Kim, S.H. Kim, H.H. Lee, K. Lee, W. Ma, X. Gong, A.J. Heeger, Adv. Mater. 18 (2006) 572–576.
- [6] C. Soci, I.W. Hwang, D. Moses, Z. Zhu, D. Waller, R. Gaudiana, C.J. Brabec, A.J. Heeger, Adv. Funct. Mater. 17 (2007) 632–636.
- [7] B.C. Thompson, J.M. Frechet, Angew. Chem. Int. Ed. 47 (2008) 58–77.
- [8] D. Cai, Q. Zheng, S.C. Chen, Q. Zhang, C.Z. Lu, Y. Sheng, D. Zhu, Z. Yin, C. Tang, J. Mater. Chem. 22 (2012) 16032–16040.
- [9] Y. Zhang, S.K. Hau, H.L. Yip, Y. Sun, O. Acton, A.K.Y. Jen, Chem. Mater. 22 (2010) 2696–2698.
- [10] J. Pei, S. Wen, Y. Zhou, Q. Dong, Z. Liu, J. Zhang, W. Tian, New J. Chem. 35 (2011) 385–393.
- [11] T.Y. Chu, J. Lu, S. Beaupré, Y. Zhang, J.R. Pouliot, J. Zhou, A. Najari, M. Leclerc, Y. Tao, Adv. Funct. Mater. 22 (2012) 2345–2351.
- [12] J.S. Moon, C.J. Takacs, S. Cho, R.C. Coffin, H. Kim, G.C. Bazan, A.J. Heeger, Nano Lett. 10 (2010) 4005–4008.
- [13] W. Ma, C. Yang, X. Gong, K. Lee, A.J. Heeger, Adv. Funct. Mater. 15 (2005) 1617–1622.
- [14] R.A. Marsh, J.M. Hodgkiss, S.A. Seifried, R.H. Friend, Nano Lett. 10 (2010) 923–930.
- [15] L. Zeng, C.W. Tang, S.H. Chen, Appl. Phys. Lett. 97 (2010) 053305.
- [16] A.H. Rice, R. Giridharagopal, S.X. Zheng, F.S. Ohuchi, D.S. Ginger, C.K. Luscombe, ACS Nano 5 (2011) 3132–3140.
- [17] Y. Zhao, Z. Xie, Y. Qu, Y. Geng, L. Wang, Appl. Phys. Lett. 90 (2007) 043504.
- [18] Y. Yao, J. Hou, Z. Xu, G. Li, Y. Yang, Adv. Funct. Mater. 18 (2008) 1783–1789.
- [19] J. Jo, S.S. Kim, S.I. Na, B.K. Yu, D.Y. Kim, Adv. Funct. Mater. 19 (2009) 866–874.
- [20] J.K. Lee, W.L. Ma, C.J. Brabec, J. Yuen, J.S. Moon, F.S. Kim, K. Lee, G.C. Bazan, A.J. Heeger, J. Am. Chem. Soc. 130 (2008) 3619–3623.
- [21] Y. Liang, Z. Xu, J. Xia, S.T. Tsai, Y. Wu, G. Li, C. Ray, L. Yu, Adv. Mater. 22 (2010) E135–E138.
- [22] Y.R. Hong, H.K. Wong, L.C. Moh, H.S. Tan, Z.K. Chen, Chem. Commun. 47 (2011) 4920–4922.
- [23] S.J. Lou, J.M. Szarko, T. Xu, L. Yu, T.J. Marks, L.X. Chen, J. Am. Chem. Soc. 133 (2011) 20661–20663.
- [24] C.V. Hoven, X.D. Dang, R.C. Coffin, J. Peet, T.Q. Nguyen, G.C. Bazan, Adv. Mater. 22 (2010) E63–E66.
- [25] M.S. Su, C.Y. Kuo, M.C. Yuan, U.S. Jeng, C.J. Su, K.H. Wei, Adv. Mater. 23 (2011) 3315–3319.
- [26] P. Ding, C. Zhong, Y. Zou, C. Pan, H. Wu, Y. Cao, J. Phys. Chem. C 115 (2011) 16211–16219.
- [27] J.M. Jiang, P.A. Yang, H.C. Chen, K.H. Wei, Chem. Commun. 47 (2011) 8877–8879.
- [28] J.M. Jiang, P.A. Yang, T.H. Hsieh, K.H. Wei, Macromolecules 44 (2011) 9155–9163.
- [29] B. Zhang, X. Hu, M. Wang, H. Xiao, X. Gong, W. Yang, Y. Cao, New J. Chem. 36 (2012) 2042–2047.
- [30] Z.G. Zhang, J. Wang, J. Mater. Chem. 22 (2012) 4178–4187.
- [31] N. Blouin, A. Michaud, D. Gendron, S. Wakim, E. Blair, R.N. Plesu, M. Belletête, G. Durocher, Y. Tao, M. Leclerc, J. Am. Chem. Soc. 130 (2008) 732–742.
- [32] M.C. Scharber, D. Mühlbacher, M. Koppe, P. Denk, C. Waldauf, A.J. Heeger, C.J. Brabec, Adv. Mater. 18 (2006) 789–794.
- [33] Y.J. Cheng, S.H. Yang, C.S. Hsu, Chem. Rev. 109 (2009) 5868–5923.
- [34] H.C. Lin, H.H. Sung, C.M. Tsai, K.C. Li, Polymer 46 (2005) 9810–9820.
- [35] J.A. Kong, E. Lim, K.K. Lee, S. Lee, S.H. Kim, Sol. Energy Mater. Solar Cells 94 (2010) 2057–2063.
- [36] J. Min, Z.G. Zhang, S. Zhang, M. Zhang, J. Zhang, Y. Li, Macromolecules 44 (2011) 7632–7638.
- [37] B. Liu, Y. Zou, B. Peng, B. Zhao, K. Huang, Y. He, C. Pan, Polym. Chem. 2 (2011) 1156–1162.
- [38] X. Chen, B. Liu, Y. Zou, L. Xiao, X. Guo, Y. He, Y. Li, J. Mater. Chem. 22 (2012) 17724–17731.
- [39] P. Piyakulawat, A. Keawprajak, K. Jirakitmongkon, M. Hanusch, J. Wlosniewski, U. Asawapirom, Sol. Energy Mater. Solar Cells 95 (2011) 2167–2172.
- [40] C.H. Chen, C.H. Hsieh, M. Dubosc, Y.J. Cheng, C.S. Hsu, Macromolecules 43 (2010) 697–708.
- [41] A. Babel, S.A. Jenekhe, J. Phys. Chem. B 107 (2003) 1749–1754.
- [42] Y. Li, Z. Li, C. Wang, H. Li, H. Lu, B. Xu, W. Tian, J. Polym. Sci. Part A: Polym. Chem. 48 (2765–2727) (2010) 2776.
- [43] J.Y. Wang, S.K. Hau, H.L. Yip, J.A. Davies, K.S. Chen, Y. Zhang, Y. Sun, A.K.Y. Jen, Chem. Mater. 23 (2011) 765–767.
- [44] D.A.M. Egbe, L.H. Nguyen, H. Hoppe, D. Mühlbacher, N.S. Sariciftci, Macromol. Rapid Commun. 26 (2005) 1389–1394.
- [45] Y.C. Kuo, M.S. Su, G.Y. Chen, C.S. Ku, H.Y. Lee, K.H. Wei, Energy Environ. Sci. 4 (2011) 2316–2322.
- [46] T. Yamamoto, B.L. Lee, Macromolecules 35 (2002) 2993–2999.
- [47] E. Wang, M. Wang, L. Wang, C. Duan, J. Zhang, W. Cai, C. He, H. Wu, Y. Cao, Macromolecules 42 (2009) 4410–4415.
- [48] M.Y. Jo, S.J. Park, T. Park, Y.S. Won, J.H. Kim, Org. Electron. 13 (2012) 2185–2191.
- [49] S. Li, B. Zhao, Z. He, S. Chen, J. Yu, A. Zhong, R. Tang, H. Wu, Q. Li, J. Qin, Z. Li, J. Mater. Chem. A 1 (2013) 4508–4515.
- [50] S.E. Shaheen, C.J. Brabec, N.S. Sariciftci, F. Padinger, T. Fromherz, J.C. Hummelen, Appl. Phys. Lett. 78 (2001) 841–843.
- [51] P. Schilinsky, U. Asawapirom, U. Scherf, M. Biele, C.J. Brabec, Chem. Mater. 17 (2005) 2175–2180.
- [52] D. Gupta, M. Bag, K.S. Narayan, Appl. Phys. Lett. 92 (2008) 093301.
- [53] J. Min, Z.-G. Zhang, S. Zhang, M. Zhang, J. Zhang, Y. Li, Macromolecules 44 (2011) 7632–7638.
- [54] M. Helgesen, S.A. Gevorgyan, F.C. Krebs, R.A.J. Janssen, Chem. Mater. 21 (2009) 4669–4675.
- [55] L. Dou, J. Gao, E. Richard, J. You, C.C. Chen, K.C. Cha, Y. He, G. Li, Y. Yang, J. Am. Chem. Soc. 134 (2012) 10071–10079.
- [56] E. Zhou, J. Cong, M. Zhao, L. Zhang, K. Hashimoto, K. Tajima, Chem. Commun. 48 (2012) 5283–5285.
- [57] Y. Liang, L. Yu, Acc. Chem. Res. 43 (2010) 1227–1236.
- [58] Z. Ma, E. Wang, K. Vandewal, M.R. Andersson, F. Zhang, Appl. Phys. Lett. 99 (2011) 143302.